Reversal of liver fibrosis by the antagonism of endocannabinoid CB1 receptor in a rat model of CCl$_4$-induced advanced cirrhosis

Ferdinando A Giannone[1,2], Maurizio Baldassarre[1,2], Marco Domenicali[1,2], Giacomo Zaccherini[1], Franco Trevisani[1], Mauro Bernardi[1,2] and Paolo Caraceni[1,2]

The endocannabinoid system is involved in the pathogenesis of liver fibrosis. Although many substances have been proved to reduce fibrosis in experimental models of chronic liver injury, most of them appear to be effective only if given as a prophylactic or early treatment. This study aimed to explore the effect of pharmacological antagonism of the endocannabinoid cannabinoid type 1 (CB1) receptor started after the stage of full-blown cirrhosis had been reached. Wistar-Han rats with carbon tetrachloride (CCl$_4$)-induced cirrhosis were randomized to receive the CB1 receptor antagonist Rimonabant (10 mg/kg/day) or the vehicle for 2 weeks. Age-matched healthy rats served as controls. Liver fibrosis was assessed using Sirius red staining, hydroxyproline concentration and α-smooth muscle actin expression. Hepatic gene expression of mediators of fibrogenesis and inflammation were evaluated by real-time PCR. We also assessed the hepatic expression of CB1 and CB2 receptors and that of the enzymes implicated in the endocannabinoid metabolism. Fibrosis was significantly reduced in rats treated with Rimonabant compared with rats receiving the vehicle. CB1 receptor antagonism limited the gene upregulation of fibrogenic and inflammatory mediators occurring in untreated cirrhotic rats. CB1 and CB2 receptor expression was increased in cirrhotic animals. Interestingly, pharmacological CB1 receptor antagonism was associated with a further induction of the CB2 receptor expression. Regression of fibrosis can be achieved by pharmacological blockade of the CB1 receptor even when started in an advanced stage of the disease. This effect is associated with the suppression of pro-fibrogenic and inflammatory mediators and may have been indirectly favoured by the induction of CB2 receptor expression.

Fibrosis results from chronic injury to the liver and the excessive accumulation of extracellular matrix (ECM) proteins. Advanced fibrotic scars disrupting the hepatic architecture and the subsequent development of nodules of regenerating hepatocytes define cirrhosis that eventually leads to liver failure and portal hypertension.

Rapidly growing knowledge on the cellular and molecular mechanisms of liver fibrosis has stimulated the search for anti-fibrotic drugs. Although many substances have been proved to reduce the accumulation of scar tissue in experimental models of chronic liver injury, most of them appear to be effective only if given as a prophylactic or early treatment. However, even advanced fibrosis is a potentially reversible phenomenon as indicated by experimental and clinical studies showing that removing the causative agent leads to a partial regression of scar tissue.[1]

In the last few years, clinical and experimental studies have demonstrated that endogenous cannabinoids (EC) participate in the complex signaling pathways that activate fibrogenic cells and contribute to ECM accumulation during chronic liver disease.[2–5] EC are lipid signaling molecules that mimic the activity of Δ9–tetrahydrocannabinol, the main psychotropic constituent of marijuana, and exert a wide range of central and peripheral effects, as they influence neuroprotection, pain and motor function, energy balance and food intake, cardiovascular function, immune and

[1]Department of Clinical Medicine, Alma Mater Studiorum University of Bologna, Bologna, Italy and [2]Center for Applied Biomedical Research (CRBA), S. Orsola-Malpighi University Hospital, Bologna, Italy

Correspondence: Professor P Caraceni, MD, Department of Clinical Medicine, U.O. Semeiotica Medica, Alma Mater Studiorum University of Bologna, Via Albertoni, 15, 40139 Bologna, Italy.
E-mail: paolo.caraceni@unibo.it

inflammatory responses, and cell proliferation. Anandamide (AEA) and 2-arachidonoylglycerol (2-AG) are the two most widely studied EC, which function mainly through interaction with two specific transmembrane G-protein-coupled receptors: cannabinoid type 1 (CB1) and type 2 (CB2) receptors.[6] AEA biosynthesis occurs from a phospholipids precursor, N-arachidonoyl-phosphatidylethanolamine (NAPE), which is hydrolyzed by a specific phospholipase D (NAPE-PLD). 2-AG is generated through the formation of a diacylglycerol (DAG) precursor starting from phospholipid molecules, which is hydrolyzed by a DAG lipase (DAGL). Degradation of AEA is mediated by the fatty acid amide hydrolase (FAAH) at the level of intracellular membranes, whereas degradation of 2-AG by monoacylglycerol lipases (MAGL) occurs in the cytosol and at the level of intracellular membranes.[6]

In mice models of liver damage induced by carbon tetrachloride (CCl_4), thiocetamide or bile duct ligation, CB1 receptor-deficient animals or animals subjected to prophylactic treatment with the CB1 receptor antagonist Rimonabant show a significantly lower deposition of fibrotic tissue than their wild-type littermates.[4] In contrast, mice invalidated for CB2 receptors present a significant increase in fibrosis following exposure to CCl_4 compared with their wild-type counterparts.[5] Taken together, these data indicate that CB1 and CB2 receptor stimulation has an opposing effect: activation of CB1 receptor promotes fibrogenesis, whereas CB2 receptor agonism triggers anti-fibrogenic responses. However, during the progression of chronic liver disease, the pro-fibrogenic CB1 signals seem to prevail over the anti-fibrogenic CB2 signals.[2,7]

As we recently observed in a study assessing sodium metabolism in pre-ascitic cirrhosis that Rimonabant treatment was associated with decreased fibrosis,[8] the present experiments were designed to determine whether pharmacological antagonism of the CB1 receptor is able to achieve the regression of fibrosis even in advanced cirrhosis when scar tissue has already been deposited. In addition, we assessed the effect of Rimonabant on the main molecular mediators implicated in the fibrogenic process.

MATERIALS AND METHODS
Animals and Experimental Design
Cirrhosis was induced by CCl_4 inhalation, as described previously,[8] in male Wistar-Han rats (Charles River Laboratories, Calco, League City, Italy) weighing 175–200 g, housed in a temperature controlled room with a 12-h light–dark cycle and given free access to tap water and pelleted rat diet (Laboratori Dottori Piccioni, Gessate, Milan, Italy) containing 2.5 g/kg of Na^+. All procedures were conducted according to the guidelines for the care and use of laboratory animals approved by our Institution.

Cirrhotic rats were studied in the pre-ascitic stage of the disease as identified by the sodium overload test (SOT),[9] which enables us to study all the animals at the same stage of cirrhosis, thereby overcoming the individual variability that, as humans, makes the rate of disease progression vary widely from rat to rat. In the present experiments, the rats became positive for SOT from the 13th to the 17th week of CCl_4 inhalation. All the rats in pre-ascitic stage presented histological features of full-blown cirrhosis and hyperdynamic circulatory syndrome.[8]

Once the SOT had been positive for 2 consecutive weeks, the rats were randomly divided into three experimental groups and killed to collect the liver samples at the following time-points:

1. Before starting treatment (CH^{Basal}; $n = 6$).
2. After 2 weeks of daily treatment by gavage with the CB1 receptor antagonist Rimonabant at a dose of 10 mg/kg dissolved in 1 ml/kg of saline solution with a drop of Tween 80 (Sigma-Aldrich, Milan, Italy; $CH^{Rimonabant}$; $n = 6$). Rimonabant was the kind gift of Dr Uberto Pagotto, University of Bologna, Italy.
3. After 2 weeks of daily administration by gavage of saline solution 1 ml/kg containing a drop of Tween 80 ($CH^{Vehicle}$; $n = 6$).

CCl_4 administration was continued during the 2-week treatment period in the $CH^{Rimonabant}$ and $CH^{Vehicle}$ groups. As Rimonabant is known to lower food intake in the short term by antagonizing the anabolic effects mediated by CB1 receptor,[10,11] we monitor the rat food intake and body weight. Although animals receiving Rimonabant tended to consume less food, the body weight after 2 weeks of treatment was not significantly different in the two groups (405 ± 16 g in treated rats *vs* 419 ± 11. Rimonabant is also known to have a psychotropic effect;[10,11] however, we did not observe an altered behavior in treated animals.

Finally, age-matched healthy rats receiving phenobarbital in the drinking water for 13–17 weeks were killed and used as a control group (CT; $n = 6$).

Analytical Methods
Histological and Biochemical Assessment of liver Fibrosis
The fibrotic area was quantified in Sirius red stained tissue section in four different fields for each slide using Image J Software (National Institutes of Health, Bethesda, MD, USA) and expressed according to the following formula (collagen area/(total area−vascular lumen area)) × 100.

Fibrosis was also assessed biochemically by the quantification of the collagen-specific amino-acid hydroxyproline as described by Jamall *et al*.[12] The liver concentration of hydroxyproline was determined from a standard curve generated from known quantities of hydroxyproline.

Assessment of Activated Hepatic Stellate Cells (HSCs) by Smooth Muscle α-Actin (α-SMA) Analysis
The activation of HSCs in the liver was evaluated using immunofluorescence, western blot and real-time PCR techniques.

Immunofluorescence. After antigen retrieval, tissue sections were incubated overnight with mouse monoclonal antibody anti-α-SMA (Dako Cytomation, Glostrup, Denmark), which was revealed using goat anti-mouse immunoglobulins conjugated to Texas Red (BioFX Laboratories, Owings Mills, MD, USA).

Western Blot. The liver tissue was homogenized in 1% Triton X-100 lysis buffer supplemented with a cocktail of protease and phosphatase inhibitors.[13] The total protein samples (40 μg) were subjected to SDS-PAGE electrophoresis, transferred to PVDF membranes (Millipore Corporation, Billerica, MA, USA) and incubated overnight with mouse anti-α-SMA antibody (1:500; Dako Cytomation). After incubation with horseradish peroxidase-conjugated anti-mouse antibody, the signals were detected by enhanced chemiluminescence with an ECL kit (Amersham Biosciences, Freiburg, Germany). Membranes were exposed to Hyperfilm ECL (Amersham Biosciences), and the densitometric analysis was performed using NIH Image-J software (National Institutes of Health).

Real-Time PCR. Total RNA from the liver tissue was extracted using Trizol/chloroform extraction (Invitrogen, Carlsbad, CA, USA) and reverse transcribed using Super-Script III RT (Invitrogen). All PCR oligonucleotide primer pairs were designed using Beacon Designer 2.0. software (Premier Biosoft International, Palo Alto, CA, USA) and then purchased from Tema Ricerche s.r.l. (San Lazzaro, BO, Italy). As internal reference, primers for β-actin and β2-micro-globulin were used. Real-time semi-quantitative PCR experiments were performed utilizing iQSybr Green Supermix (BioRad, Richmond, CA, USA) in the iCycler (BioRad) instrument. The fold changes in gene expression relative to the levels obtained in healthy rats, which were considered equal to 1, were analyzed and calculated with the $2^{-\Delta\Delta Ct}$ method.[14]

Assessment of Hepatic Expression of Molecular Mediators of Fibrogenesis

Liver gene expression for transforming growth factor-β (TGF-β), platelet-derived growth factor (PDGF), collagen type-1α1 (Col-1α1), tissue inhibitor of metalloproteinase-1 (TIMP-1), matrix metalloproteinases (MMPs; 1, 2, 8, 9 and 13), tumor necrosis factor-α (TNF-α), monocyte chemotactic protein-1 (MCP-1), interleukin-10 (IL-10) and suppressor of cytokine signaling-3 (SOCS3), inducible nitric oxide synthase (iNOS), and endothelin-1 (ET-1) was performed by real-time PCR as described above (see Supplementary Material for the primer sequences).

Finally, TGF-β (1:500, Millipore Corporation) and MMP-13 (1:500, Millipore Corporation) protein expressions were evaluated by using western blot techniques as described above.

Assessment of MMPs Activity

MMPs activity in the liver was evaluated by using the Zymogram of protease activity.[15] Briefly, lysates of liver tissue were loaded on 10% polyacrylamide gels supplemented with 0.1% gelatine in standard SDS loading buffer containing 0.1% SDS. Gels were run at 200 V for 1 h at 4°C in a Bio-Rad Mini-Protean apparatus (BioRad) and then soaked in 200 ml of 25% Triton X-100 solution in a shaker for 1 h. Then, the gels were immersed in a reaction buffer for 72 h at 37°C and stained with Coomassie brilliant blue. After staining, gels were destained until clear bands were visible on the dark background.

Assessment of Hepatic Expression of EC CB1 and CB2 Receptors

Expression of EC CB1 and CB2 receptors in the liver was evaluated by immunohistochemistry, real-time PCR and western blot techniques.

Immunohistochemistry. After antigen retrieval, liver tissue sections were incubated with rabbit polyclonal anti-CB1 receptor antibody (1:100; Affinity BioReagents, Golden, CO, USA) and anti-CB2 receptor antibody (1:100; Abcam, Cambridge, UK). The primary antibody was revealed using peroxidase-conjugated goat anti-rabbit immunoglobulins (EnVision, Dako Cytomation), using 3′,3′-diaminobenzidine (Sigma-Aldrich, St Louis, MO, USA).

Real-Time PCR. Evaluation of hepatic mRNA expression of CB1 and CB2 receptor was performed by real-time PCR as described above (see Supplementary Material for the primer sequences).

Western Blot. Hepatic CB1 and CB2 receptor protein expression was evaluated using rabbit polyclonal anti-CB1 receptor antibody (1:500; Affinity BioReagents) and anti-CB2 receptor antibody (1:500; Abcam) by western blot technique as described above.

Assessment of Hepatic Gene Expression of Enzymes Implicated in EC Metabolism

Last, we assessed the hepatic gene expression of the enzymes implicated in the synthesis and degradation of AEA and 2-AG. The hepatic gene expression of NAPE-PLD, FAAH, DAGL and MAGL was measured by real-time PCR as described above (see Supplementary Material for the primer sequences).

Statistical Analysis

Statistical analysis was performed using one-way ANOVA with Bonferroni's correction for multiple comparisons. All data are expressed as mean ± s.e.m., and they are considered significant at a *P* level of 0.05 or less as mean. Calculations were performed using SPSS 11.0 software (SPSS, Chicago, IL, USA).

RESULTS
Hepatic Fibrosis and Activation of HSC

When included in the study, all CCl₄-treated rats were in the pre-ascitic stage of the disease (CH^Basal), presenting a liver with a finely granulated surface, histological features of full-blown cirrhosis, and a significantly higher fibrosis score and

hydroxyproline content than healthy rats. After 2 weeks, rats receiving the vehicle showed a similar histology, extent of fibrosis and hydroxyproline content compared with CH[Basal] By contrast, rats treated with the CB1 receptor antagonist displayed thinner and incomplete septa and significantly less fibrosis and hydroxyproline than the other cirrhotic groups (Figure 1). No appreciable histological alterations could be identified in healthy rats (CT; Figure 1).
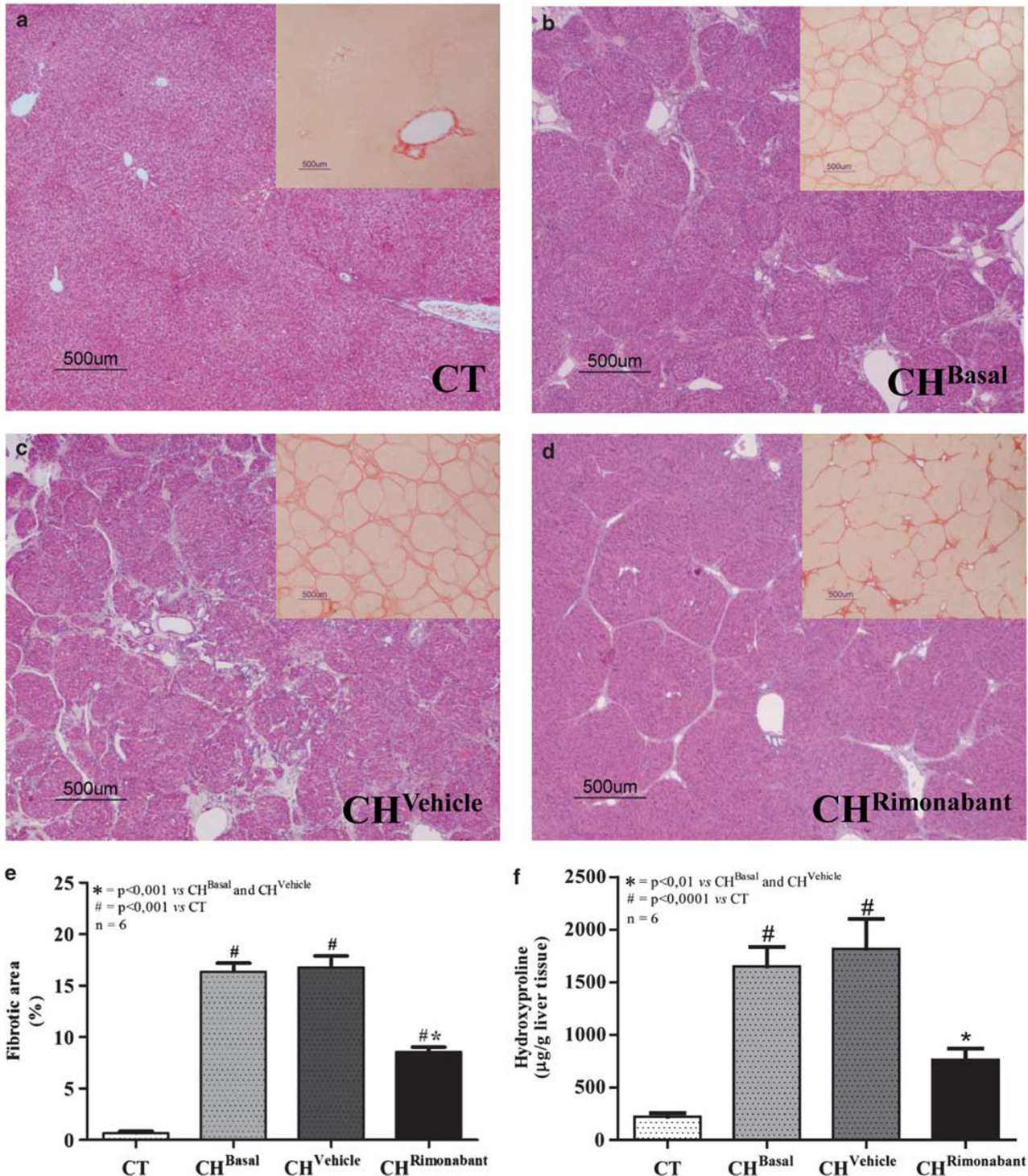
Figure 1 Hepatic fibrosis. (**a–d**) Representative images of H&E-stained liver sections (× 40) from healthy rats (CT), pre-ascitic cirrhotic rats (CH[Basal]) and rats receiving the vehicle (CH[Vehicle]) or 10 mg/kg/day of the cannabinoid type 1-antagonist Rimonabant (CH[Rimonabant]) for 2 additional weeks. Representative images of Sirius Red stained liver section are inserted in the upper right corner of each panel. (**e**) Quantification of the fibrotic area expressed as percent of the total area. (**f**) Hepatic hydroxyproline tissue content. Data are expressed as mean ± s.e.

HSC activation was evaluated by assessing the expression of the well-validated marker α-SMA. As expected, CH[Basal] rats showed a marked induction of α-SMA gene and protein expression and immunofluorescence was highly positive in the portal tracts and fibrous septa. Although no significant differences were seen in CH[Vehicle] rats, treatment with the CB1 receptor antagonist was associated with a blunted α-SMA expression and a weaker immunofluorescent staining

(Figure 2). Accordingly, the gene expression of Col-1α1, main component of ECM produced by activated HSC, showed a similar pattern (Figure 2).

Expression of Molecules Implicated in ECM Remodeling
As expected, CH[Basal] rats showed a pro-fibrogenic pattern consisting of upregulation of the TIMP-1(Figure 3) associated to the elevation of the major metalloproteases (MMPs;
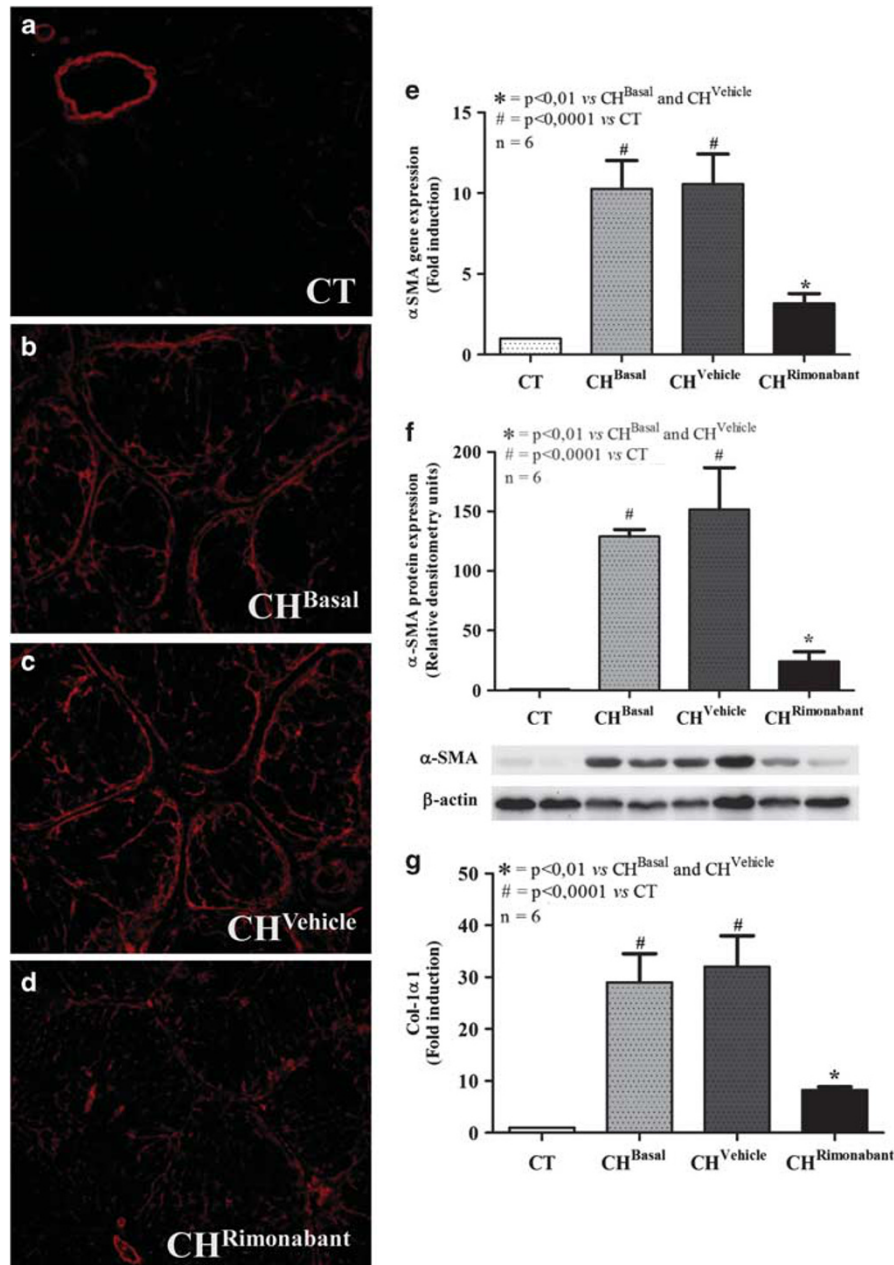
Figure 2 Hepatic smooth muscle α-actin (α-SMA) and collagen type-1α1 (Col-1α1). (**a–d**) Representative images of α-SMA immunofluorescence stained liver sections (× 40) from healthy rats (CT), pre-ascitic cirrhotic rats (CH[Basal]) and rats receiving the vehicle (CH[Vehicle]) or 10 mg/kg/day of the cannabinoid type 1-antagonist Rimonabant (CH[Rimonabant]) for 2 additional weeks. (**e**) Hepatic gene expression of α-SMA. Values were determined by real-time PCR and expressed as fold induction over control healthy rats. (**f**) Densitometric quantification (upper) and representative image (lower) of western blot analysis of hepatic α-SMA protein expression. (**e**) Hepatic gene expression of Col-1α1. Values were determined by real-time PCR and expressed as fold induction over control healthy rats. Data are expressed as mean ± s.e.

gelatinases and collagenases) that can be considered a compensatory mechanism in response to the increased scar tissue (Figure 4a). Again, while no significant differences were found in CH^{Vehicle} rats, treatment with CB1 receptor antagonist induced an almost complete suppression of TIMP-1 induction (Figure 3) and reduced MMP upregulation
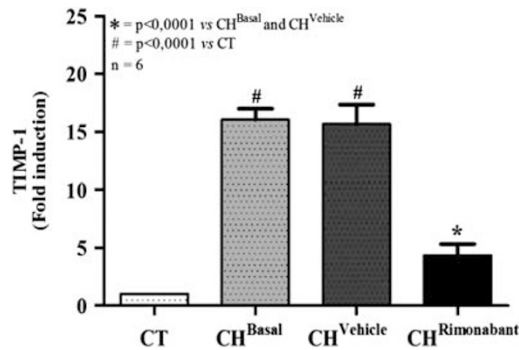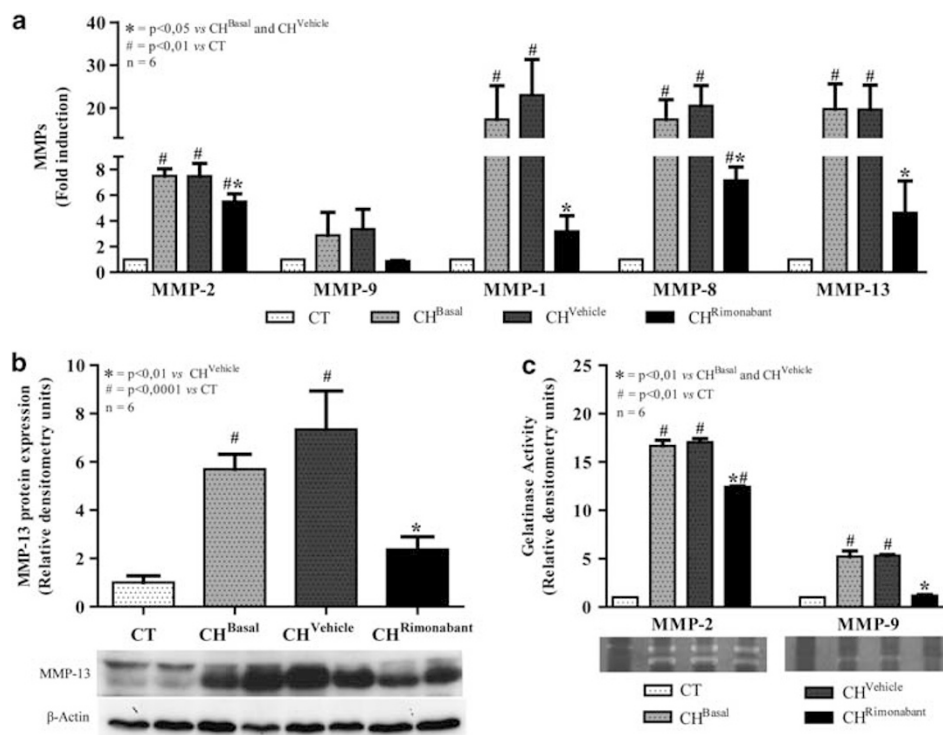

Figure 3 Hepatic TIMP-1. Hepatic gene expression of tissue inhibitor of metalloproteinase-1 (TIMP-1) in healthy rats (CT), in pre-ascitic cirrhotic rats (CH^{Basal}) and in rats receiving the vehicle (CH^{Vehicle}) or 10 mg/kg/day of the cannabinoid type 1-antagonist Rimonabant (CH^{Rimonabant}) for 2 additional weeks. Values were determined by real-time PCR and expressed as fold induction over control healthy rats. Data are expressed as mean ± s.e.

(Figure 4a). Finally, the specific activity of the MMP-2 and MMP-9 assessed by gelatin zymography, and the protein expression of MMP-13, member of the collagenase family, assessed by western blot, confirmed the data obtained in real-time PCR (Figures 4b and c).
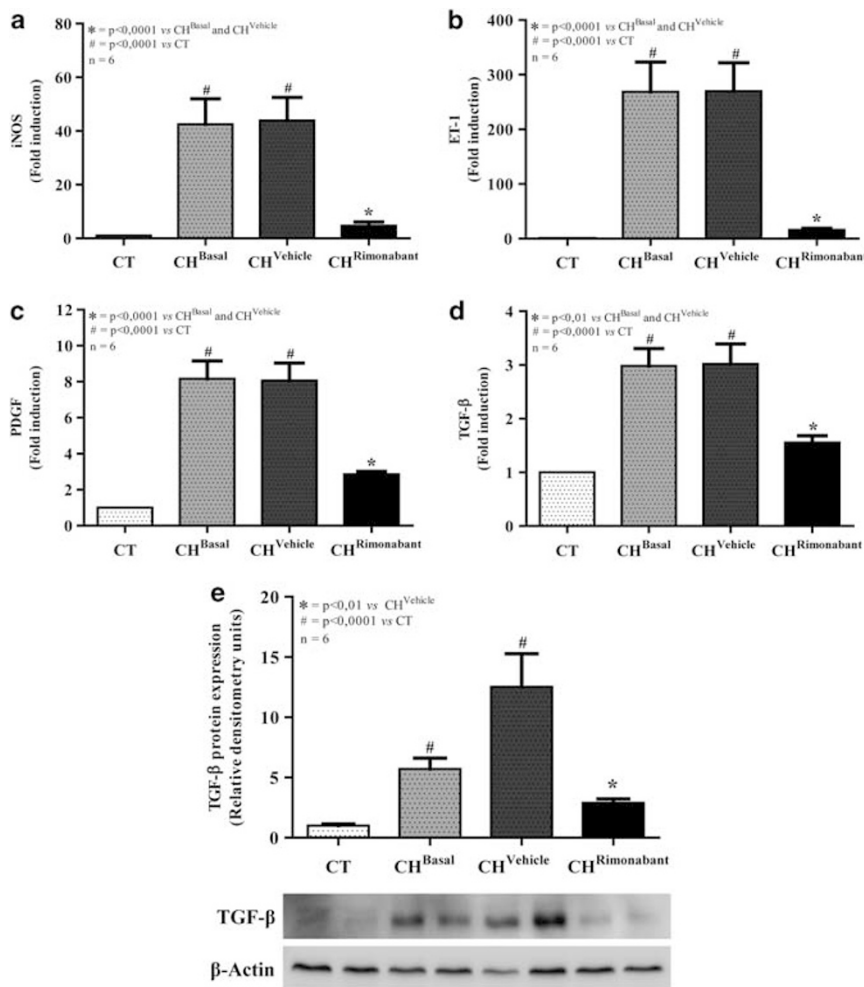
Expression of Mediators Implicated in the Fibrogenic Process

Cirrhotic rats at the pre-ascitic stage of the disease showed the expected hepatic gene upregulation of TGF-β and PDGF, which induce HSC activation and proliferation, and iNOS and ET-1, which contribute to the inflammatory response and vascular flow disarrangement (Figures 5a–d). Although a similar pattern of induction was observed in cirrhotic CH^{Vehicle} rats, the gene expression of all these pro-fibrogenic mediators was blunted by Rimonabant treatment (Figures 5a–d). We also assessed by western blot analysis the hepatic protein content of TGF-β, which was also significantly reduced by the CB1 receptor antagonism (Figure 5e).

We then analyzed the hepatic gene expression of the pro-inflammatory and chemotactic mediators TNF-α and MCP-1. Again, treatment with Rimonabant abolished the upregulation observed in CH^{Vehicle} and CH^{Basal} rats (Figures 6a and b). Finally, we found in untreated cirrhotic rats a significant downregulation of the anti-inflammatory cytokine IL-10,

Figure 4 Hepatic expression of matrix metalloproteinases. (**a**) Hepatic gene expression of matrix metalloproteinases (MMPs; 2, 9, 1, 8 and 13) in healthy rats (CT), in pre-ascitic cirrhotic rats (CH^{Basal}) and in rats receiving the vehicle (CH^{Vehicle}) or 10 mg/kg/day of the cannabinoid type 1-antagonist Rimonabant (CH^{Rimonabant}) for 2 additional weeks. Values were determined by real-time PCR and expressed as fold induction over control healthy rats. (**b**) Densitometric quantification (upper) and representative image (lower) of western blot analysis of hepatic MMP-13. (**c**) Densitometric quantification of MMP-2 and MMP-9 activity (upper) and their representative zymogram (lower). Data are expressed as mean ± s.e.

Figure 5 Hepatic expression mediators implicated in the fibrogenic process. Hepatic gene expression of (**a**) inducible nitric oxide synthase (iNOS), (**b**) endothelin 1 (ET-1), transforming growth factor-β (TGF-β), (**c**) platelet-derived growth factor (PDGF) and (**d**) monocyte chemotactic protein-1 (MCP-1), in healthy rats (CT), in pre-ascitic cirrhotic rats (CH^{Basal}) and in rats receiving the vehicle (CH^{Vehicle}) or 10 mg/kg/day of the cannabinoid type 1-antagonist Rimonabant (CH^{Rimonabant}) for 2 additional weeks. Values were determined by real-time PCR and expressed as fold induction over control healthy rats. (**e**) Densitometric quantification (upper) and representative image (lower) of western blot analysis of hepatic transforming growth factor-β (TGF-β). Data are expressed as mean ± s.e.

which was reversed by administration of the CB1 receptor antagonist (Figure 6c). Interestingly, Rimonabant induced the gene upregulation of SOCS3, which has a major role in the negative regulatory signaling pathways of pro-inflammatory cytokines (Figure 6d).

Expression of CB Receptors and Enzymes Implicated in the EC Metabolism

The protein and gene expressions of CB1 and CB2 receptors were clearly upregulated in the liver of pre-ascitic cirrhotic rats, and a positive immunostaining was revealed along the fibrotic and periportal area. A similar pattern of expression was found in CH^{Vehicle} rats. Although no significant differences were observed for the CB1 receptor, the 2-week treatment with Rimonabant induced a significantly increased expression of the CB2 receptor (Figures 7 and 8). The specificity of the

staining was verified by omitting the primary antibody as negative controls (see Supplementary Material).

Last, we assessed the gene expression of the enzymes implicated in the metabolism of the two major EC, the AEA and 2-AG. Although the expression of the synthetic enzymes NAPE-PLD and DAGL was similar in all groups, the degradative enzymes FAAH and MAGL were downregulated in pre-ascitic rats, indicating the possibility of an increased EC content in the cirrhotic liver. After 2 weeks, FAAH and MAGL downregulation was partially reverted in rats treated with Rimonabant, but not in those receiving the vehicle (Figure 9).

DISCUSSION

The EC system contributes to ECM deposition during chronic liver diseases, the CB1 receptor being pro-fibrogenic
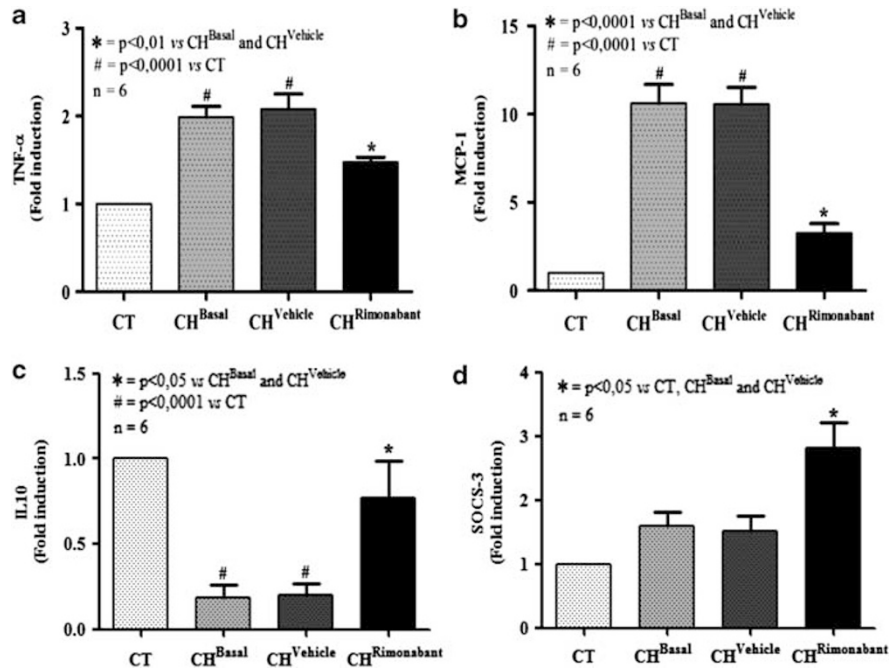
Figure 6 Hepatic expression of pro- and anti-inflammatory molecules implicated in the fibrogenic process. Hepatic gene expression of (**a**) tumor necrosis factor-α (TNF-α), (**b**) monocyte chemotactic protein-1 (MCP-1), (**c**) interleukin-10 (IL-10) and (**d**) suppressor of cytokine signaling-3 (SOCS3) in healthy rats (CT), in pre-ascitic cirrhotic rats (CH^{Basal}) and in rats receiving the vehicle (CH^{Vehicle}) or 10 mg/kg/day of the cannabinoid type 1-antagonist Rimonabant (CH^{Rimonabant}) for 2 additional weeks. Values were determined by real-time PCR and expressed as fold induction over control healthy rats. Data are expressed as mean ± s.e.
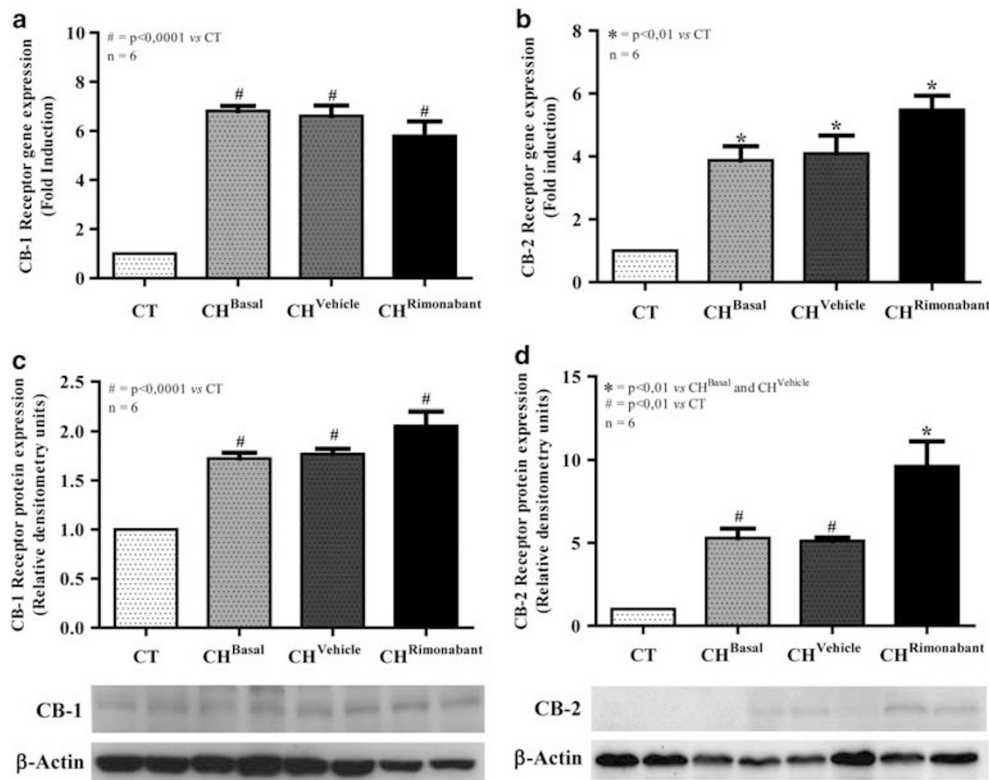
Figure 7 Hepatic expression of cannabinoid type 1 (CB1) and CB2 receptors. (**a**, **b**) Hepatic CB1 and CB2 receptor gene expression and (**c**, **d**) densitometric quantification (upper) plus representative images (lower) of western blot analysis of CB1 and CB2 receptor protein expression in healthy rats (CT), in pre-ascitic cirrhotic rats (CH^{Basal}) and in rats receiving the vehicle (CH^{Vehicle}) or 10 mg/kg/day of the CB1-antagonist Rimonabant (CH^{Rimonabant}) for 2 additional weeks. Data are expressed as mean ± s.e.
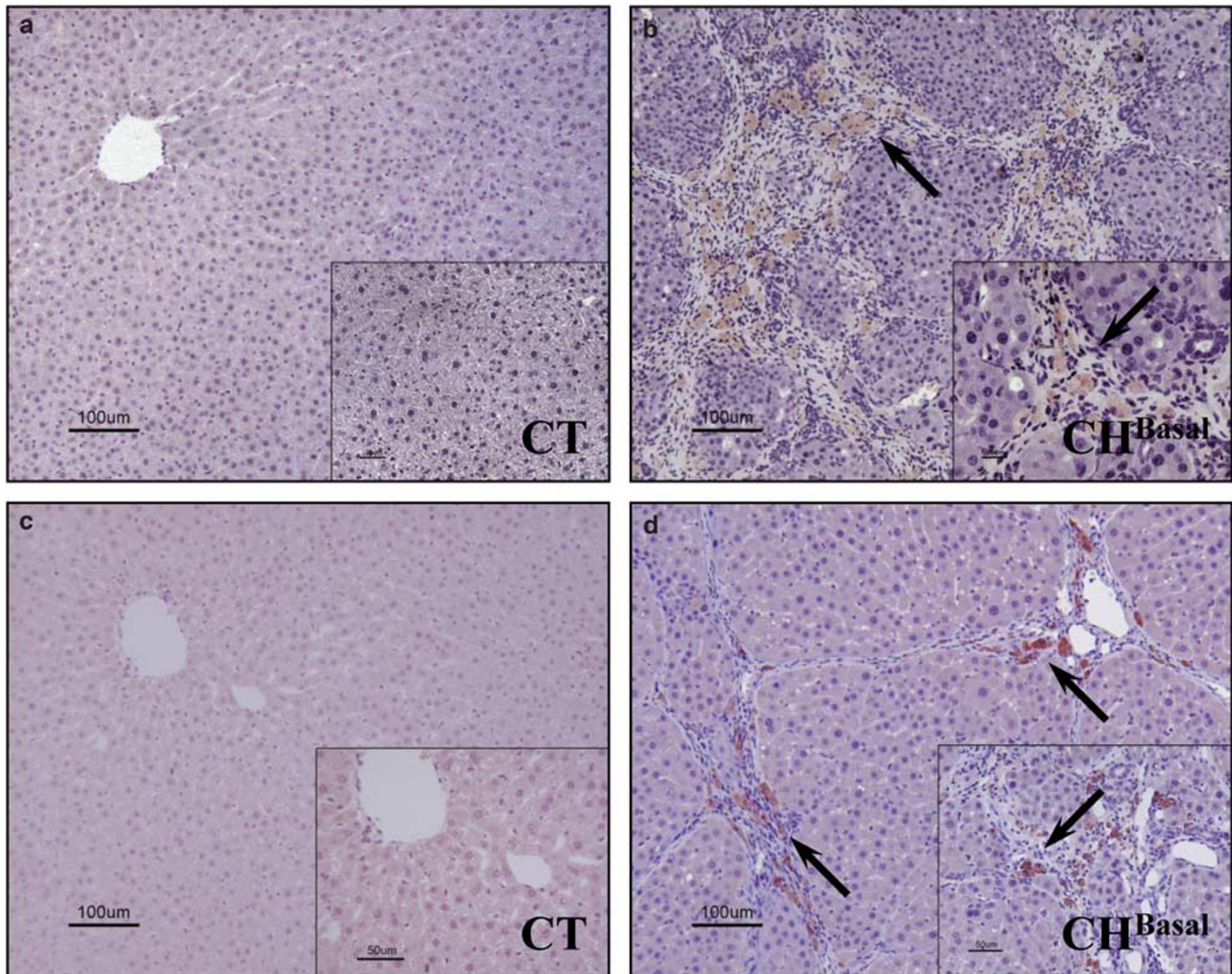
Figure 8 Immunostaining of hepatic cannabinoid type 1 (CB1) and CB2 receptors. Representative images of CB1 and CB2 receptor immunostained liver sections ($\times$ 20 outer and $\times$ 40 inner) from healthy control rats (CT; **a**, **c**) and pre-ascitic cirrhotic rats (CH$^{\text{Basal}}$; **b**, **d**).

and the CB2 receptor being anti-fibrogenic.[4,5] This study demonstrates that the pharmacological antagonism of the CB1 receptor is able to revert fibrosis even when the advanced stage of full-blown cirrhosis has been reached and the fibrogenic insult (ie, CCl$_4$ administration) is maintained. This timing of administration represents a major difference and a novelty with respect to previously published experiments showing that ECM deposition can be markedly lowered when the CB1 receptor antagonist is given as a prophylactic treatment.[4]

Regardless of the underlying etiology, quiescent HSC gain a myofibroblast-like phenotype in response to chronic liver injury and/or inflammation, acquiring proliferative, pro-inflammatory and contractile properties. The most striking response of activated HSC is excessive collagen synthesis associated with reduced ECM degradation. The perpetuation of this pro-inflammatory and pro-fibrogenic background, mediated by the interplay of a long series of paracrine and autocrine molecules, ultimately replaces the normal liver architecture with fibrotic tissue and regenerative parenchymal nodules.[16,17]

Our experiments indicate that CB1 receptor antagonism exerts its anti-fibrogenic effect by acting at different steps of this vicious cycle. The number of activated HSC is significantly reduced after Rimonabant treatment as shown by the analysis of α-SMA expression, a well-accepted marker of hepatic myofibroblasts. This is consistent with previous observations that activated HSC undergo apoptosis during treatment with the CB1 receptor antagonist.[4] Although *in vitro* and *in vivo* studies investigating the relationship among EC, CB receptors and HSC death (apoptosis or necrosis) have produced conflicting results,[2,18,19] the CB1 receptor has been suggested to mediate cytoprotective pathways deactivated by its antagonism.[4]

Beside HSC, biliary cells represent an other potential target of EC during fibrogenesis.[20–21] In our non-cholestatic model, biliary cells proliferate along the fibrotic septa in cirrhotic livers as shown by the immunostaining for the specific CK-19
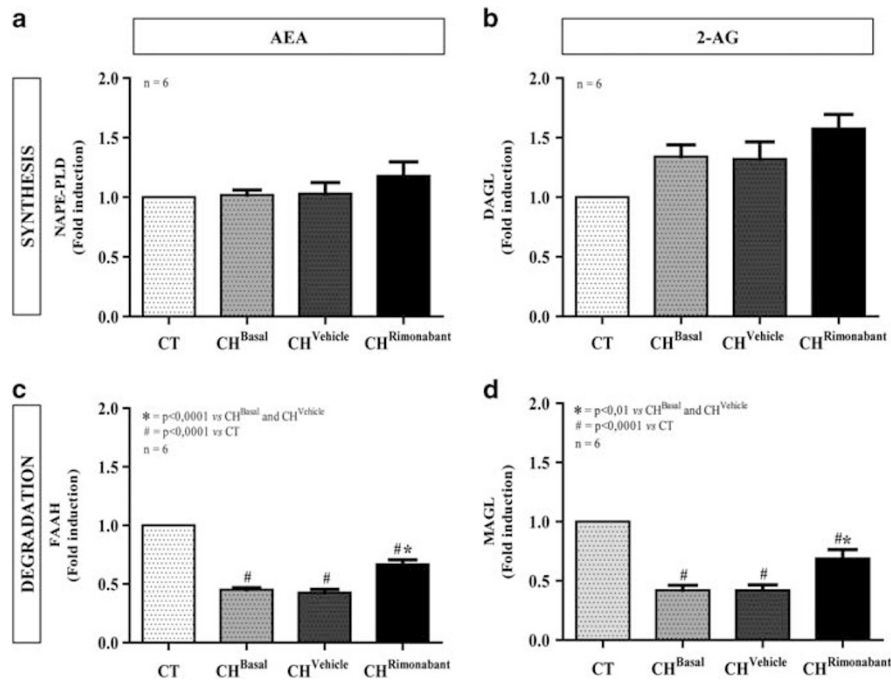
Figure 9 Hepatic expression of enzymes implicated in the ananadamide (AEA) (**a** and **c**) and 2-acylglycerol (2-AG) (**b** and **d**) metabolism. Hepatic gene expression of (**a**) arachidonoyl-phosphatidylethanolamine phospholipase D (NAPE-PLD; AEA synthesis), (**b**) fatty acid amide hydrolase (FAAH; AEA degradation), (**c**) diacylglycerol lipase (DAGL; 2-AG synthesis) (**d**) and monoacylglycerol lipases (MAGL; 2-AG degradation) in healthy rats (CT), in pre-ascitic cirrhotic rats (CH^{Basal}) and in rats receiving the vehicle (CH^{Vehicle}) or 10 mg/kg/day of the CB1-antagonist Rimonabant (CH^{Rimonabant}) for 2 additional weeks. Values were determined by real-time PCR and expressed as fold induction over control healthy rats. Data are expressed as mean ± s.e.

biliary marker (see Supplementary Material). However, the reduced immunostaining that was observed after Rimonabant treatment likely results from the improvement of the liver architecture and function rather than from the direct effect of CB1 receptor antagonism on the biliary cells.

This study clearly indicates that antagonism of the CB1 receptor interferes with the production of several pro-fibrogenic, pro-inflammatory and anti-inflammatory mediators secreted in the liver during chronic liver injury and the wound healing process. Among growth factors, TGF-β favours the transition of quiescent HSC to myofibroblast-like cells, stimulates the synthesis of ECM proteins and inhibits their degradation, although PDGF is the most potent mitogen for HSC.[16,17]

ET-1 represents the major contractile stimulus toward HSC, which in part is autocrine derived.[16,17] Contraction of myofibroblasts localized around the liver sinusoids may increase intrahepatic vascular resistance and ultimately portal hypertension.[22,23] Moreover, the NO generated by the activity of the inducible form of NO synthase, which is highly responsive to pro-inflammatory cytokines and endotoxemia, has been proposed to induce liver damage and facilitate the deposition of collagen.[24]

TNF-α and MCP-1 have an important role in the development of fibrosis as pro-inflammatory molecules contributing to the activation of HSC and to the recruitment of myofibroblasts, macrophages and other effector cells to sites of

tissue injury.[16,17] As we have recently showed in a model of acute liver injury produced by ischemia-reperfusion complicated by endotoxemia,[13] Rimonabant appears to exert its protective activity also by promoting the synthesis of IL-10 and SOCS-3. IL-10 is a major anti-inflammatory cytokines, which restrains the immune response under various stimuli[25,26] and may reduce fibrogenesis by downregulating pro-fibrogenic cytokines, including TGF-β and TNF-α[27] and fibrogenetic mediators, such as TIMP-1.[28,29] It has been also proposed that IL-10 is able to inhibit HSC activation and to promote their apoptosis during liver fibrogenesis.[28,29] Beside its well-known interference with the pro-inflammatory cytokine signaling pathways,[30,31] SOCS3 has been found to negatively regulate fibrogenesis in the liver[32,33] and to suppress the signaling molecule STAT3, which activates TGF-β transcription.[32]

Our data demonstrate that the hepatic expression of all these molecules are deeply affected in cirrhosis leading to a pro-fibrogenic environment, which is fully counteracted by CB1 receptor antagonism.

Pharmacological inhibition of the CB1 receptor also appears to affect the synthesis of molecules implicated in ECM remodeling. The net deposition of scar tissue depends on the balance between synthesis and degradation, the latter reflecting the relative activity of MMPs and their inhibitor TIMPs primarily produced by HSC and other inflammatory cells.[16,17] In experimental and human cirrhosis, fibrosis appears to be the result not only of excessive ECM synthesis,

but also of reduced degradation, which is caused by the up-regulation of TIMPs inactivating the concurrently secreted MMPs.[16,17,34–36] According to this mechanism, untreated cirrhotic rats in our experiments presented not only a marked induction of Col-1α1 gene expression, but also a significant upregulation of the MMPs, which can be explained as a compensatory mechanism designed to eliminate excess scar tissue.[16] However, the concomitant TIMP-1 induction over-whelmed MMPs activity, thus leading to a net ECM deposition in the liver.

Treatment with the CB1 receptor antagonist was associated with a marked reduction of Col-1α1 and TIMP-1 gene expression, apparently in agreement with the partial regression of fibrosis. More controversial is the result regarding the expression of MMPs as one would expect higher MMP expression/activity during fibrosis resolution. However, several evidences can render understandable our finding. First, it has been shown that the MMPs expression, which is upregulated in fibrotic liver, remains elevated in the early phase of fibrosis regression to decline thereafter in parallel with the recovery of liver tissue.[37] Thus, in our study, it can be speculated that the MMPs levels were not as high as theoretically expected as they were measured when fibrosis was already resolved to a significant extent. Furthermore, the finding of low MMPs levels after fibrosis regression has been previously reported by other investigators.[37–40] As in our study, low MMPs expression was associated with loss of activated HSCs and reduced TGF-β.[37,38,41–43] Finally, as during fibrogenesis, it can be anticipated that the leading role to fibrosis reabsorption would be performed by TIMP-1 expression, the fall of which would unmasks the MMP activity.[16,39,41]

There is a general consensus that the EC system is activated during cirrhosis.[4,5,44–48] Accordingly, our untreated cirrhotic rats had a significant upregulation of CB1 and CB2 receptors along fibrotic septa and portal tracts where maximal is the presence of activated HSC expressing the CB receptors, as reported by other authors in rats and humans.[4,5,45–47] Furthermore, the downregulation of the enzymes responsible for EC degradation, FAAH and MAGL, represents indirect evidence of increased hepatic EC levels in cirrhotic livers.

It is well accepted that activation of CB1 receptor promotes fibrogenesis, while CB2 receptor agonism triggers anti-fibrogenic responses in the liver. However, in chronic liver diseases, the pro-fibrogenic CB1 signals prevails on the anti-fibrogenic CB2 signals, supporting the use of CB1 antagonists. Nonetheless, the stimulation of CB2 receptor has been shown to have an anti-fibrogenic effect by inducing apoptosis or growth arrest in activated HSCs.[18,19,45] Interestingly, in our study, CB2 receptor expression increased following Rimonabant treatment, whereas that of the CB1 receptor remained unchanged. Although this finding remains unexplained, it is tempting to speculate that by blocking the CB1 receptor, more EC will be available to interact with the CB2 receptor, thus promoting in a positive loop its expression and its anti-inflammatory and anti-fibrogenic properties.

The finding that Rimonabant attenuates the expression of EC degradative enzymes, thereby favouring their clearance in the liver, is even more intriguing, as in vitro studies indicate that both AEA and 2-AG are able to trigger the death of activated HSC through mechanisms other than the interaction with CB receptors.[3,18,19] Clearly, much experimental work is still needed to unveil the true role of EC or other CB receptor ligands in the process of fibrogenesis.

Experimental evidence has consistently demonstrated that Rimonabant improves hyperdynamic circulation, cirrhotic cardiomiopathy and hepatic encephalopathy, and delays ascitic decompensation.[2] For this reason, pharmacological CB1 receptor antagonism has already been advocated as a potential novel treatment in advanced cirrhosis. Unfortunately, the centrally mediated side effects, anxiety and depression being the most clinically relevant, preclude the clinical use of Rimonabant and other class-related compounds. However, the results of our study represent a further reason to develop CB1 receptor antagonists with a restricted access to the central nervous system, thus avoiding negative psychotropic actions,[49] and investigate their application in the setting of liver cirrhosis.

In conclusion, regression of fibrosis can be achieved by the pharmacological blockade of CB1 receptor antagonism even in an advanced stage of the disease when full-blown cirrhosis has already developed. This effect is associated with the suppression of a series of pro-fibrogenic and inflammatory mediators and may have been indirectly favoured by the induction of CB2 receptor expression.

Supplementary Information accompanies the paper on the Laboratory Investigation website (http://www.laboratoryinvestigation.org)

DISCLOSURE/CONFLICTS OF INTEREST
The authors declare no conflicts of interest.

1. Bataller R, Brenner DA. Liver fibrosis. J Clin Invest 2005;115:209–218.
2. Siegmund SV, Schwabe RF. Endocannabinoids and liver disease. II. Endocannabinoids in the pathogenesis and treatment of liver fibrosis. Am J Physiol Gastrointest Liver Physiol 2008;294:G357–G362.
3. Hézode C, Roudot-Thoraval F, Nguyen S, et al. Daily cannabis smoking as a risk factor for fibrosis progression in chronic hepatitis C. Hepatology 2005;42:63–71.
4. Teixeira-Clerc F, Julien B, Grenard P, et al. CB1 cannabinoid receptor antagonism: a new strategy for the treatment of liver fibrosis. Nat Med 2006;12:671–676.
5. Julien B, Grenard P, Teixeira-Clerc F, et al. Antifibrogenic role of the cannabinoid receptor CB2 in the liver. Gastroenterology 2005;128:742–755.
6. De Petrocellis L, Di Marzo V. An introduction to the endocannabinoid system: from the early to the latest concepts. Best Pract Res Clin Endocrinol Metab 2009;23:1–15.
7. Caraceni P, Domenicali M, Giannone F, et al. The role of the endocannabinoid system in liver diseases. Best Pract Res Clin Endocrinol Metab 2009;23:65–77.

8. Domenicali M, Caraceni P, Giannone F, et al. Cannabinoid type 1 receptor antagonism delays ascites formation in rats with cirrhosis. Gastroenterology 2009;137:341–349.

9. Domenicali M, Caraceni P, Principe A, et al. A novel sodium overload test predicting ascites decompensation in rats with CCl₄-induced cirrhosis. J Hepatol 2005;43:92–97.

10. Pacher P, Bátkai S, Kunos G. The endocannabinoid system as an emerging target of pharmacotherapy. Pharmacol Rev 2006;58:389–462.

11. Li C, Jones PM, Persaud SJ. Role of the endocannabinoid system in food intake, energy homeostasis and regulation of the endocrine pancreas. Pharmacol Ther 2011;129:307–320.

12. Jamall IS, Finelli VN, Que Hee SS. A simple method to determine nanogram levels of 4-hydroxyproline in biological tissues. Anal Biochem 1981;112:70–75.

13. Caraceni P, Pertosa AM, Giannone F, et al. Antagonism of the cannabinoid CB-1 receptor protects rat liver against ischaemia-reperfusion injury complicated by endotoxaemia. Gut 2009;58:1135–1143.

14. Kenneth J, Livak, Thomas D. Schmittgen. Analysis of relative gene expression data using real-time quantitative PCR and the 2-[Delta][Delta]CT method. Methods 2001;25:402–408.

15. Mandal M, Das S, Chakraborti T, et al. Role of matrix metalloprotease-2 in oxidant activation of Ca² ATPase by hydrogen peroxide in pulmonary vascular smooth muscle plasma membrane. J Biosci 2003;28:205–213.

16. Iredale P.J. Models of liver fibrosis: exploring the dynamic nature of inflammation and repair in a solid organ. J Clin Invest 2007;117:539–548.

17. Friedman SL. Hepatic stellate cells: protean, multifunctional, and enigmatic cells of the liver. Physiol Rev 2008;88:125–172.

18. Siegmund SV, Qian T, De Minicis S, et al. The endocannabinoid 2-arachidonoyl glycerol induces death of hepatic stellate cells via mitochondrial reactive oxygen species. FASEB J 2007;21:2798–2806.

19. Siegmund SV, Uchinami H, Osawa Y, et al. Anandamide induces necrosis in primary hepatic stellate cells. Hepatology 2005;41:1085–1095.

20. Lowes KN, Brennan BA, Yeoh GC, et al. Oval cell numbers in human chronic liver diseases are directly related to disease severity. Am J Pathol 1999;154:537–541.

21. Richardson MM, Jonsson JR, Powell EE, et al. Progressive fibrosis in nonalcoholic steatohepatitis: association with altered regeneration and a ductular reaction. Gastroenterology 2007;133:80–90.

22. Pinzani M, Milani S, De FR, et al. Endothelin 1 is overexpressed in human cirrhotic liver and exerts multiple effects on activated hepatic stellate cells. Gastroenterology 1996;110:534–548.

23. Feng HQ, Weymouth ND, Rockey DC. Endothelin antagonism in portal hypertensive mice: implications for endothelin receptor-specific signaling in liver disease. Am J Physiol Gastrointest Liver Physiol 2009;297:G27–G33.

24. Aram G, Potter JJ, Liu X, et al. Lack of inducible nitric oxide synthase leads to increased hepatic apoptosis and decreased fibrosis in mice after chronic carbon tetrachloride administration. Hepatology 2008;47:2051–2058.

25. Asadullah K, Sterry W, Volk HD. Interleukin-10 therapy - review of a new approach. Pharmacol Rev 2003;55:241–269.

26. Grütz G. New insights into the molecular mechanism of interleukin-10-mediated immunosuppression. J Leukoc Biol 2005;77:3–15.

27. Louis H, Van Laethem JL, Wu W, et al. Interleukin-10 controls neutrophilic infiltration, hepatocyte proliferation, and liver fibrosis induced by carbon tetrachloride in mice. Hepatology 1998;28:1607–1615.

28. Zhang LJ, Chen YX, Chen ZX, et al. Effect of interleukin-10 and platelet-derived growth factor on expressions of matrix metalloproteinases-2 and tissue inhibitor of metalloproteinases-1 in rat fibrotic liver and cultured hepatic stellate cells. World J Gastroenterol 2004;10:2574–2579.

29. Zhang LJ, Zheng WD, Shi MN, et al. Effects of interleukin-10 on activation and apoptosis of hepatic stellate cells in fibrotic rat liver. World J Gastroenterol 2006;12:1918–1923.

30. O'Sullivan LA, Liongue C, Lewis RS, et al. Cytokine receptor signaling through the Jak-Stat-Socs pathway in disease. Mol Immunol 2007;44:2497–2506.

31. Mair M, Blaas L, sterreicher CH, et al. JAK-STAT signaling in hepatic fibrosis. Front Biosci 2011;17:2794–2811.

32. Ogata H, Chinen T, Yoshida T, et al. Loss of SOCS3 in the liver promotes fibrosis by enhancing STAT3-mediated TGF-beta1 production. Oncogene 2006;25:2520–2530.

33. Niwa Y, Kanda H, Shikauchi Y, et al. Methylation silencing of SOCS-3 promotes cell growth and migration by enhancing JAK/STAT and FAK signalings in human hepatocellular carcinoma. Oncogene 2005;24:6406–6417.

34. Arthur MJ. Fibrogenesis II. Metalloproteinases and their inhibitors in liver fibrosis. Am J Physiol Gastrointest Liver Physiol 2000;279:G245–G249.

35. Iredale JP, Benyon RC, Arthur MJ, et al. Tissue inhibitor of metalloproteinase-1 messenger RNA expression is enhanced relative to interstitial collagenase messenger RNA in experimental liver injury and fibrosis. Hepatology 1996;24:176–184.

36. Benyon RC, Iredale JP, Goddard S, et al. Expression of tissue inhibitor of metalloproteinases 1 and 2 is increased in fibrotic human liver. Gastroenterology 1996;110:821–831.

37. Zhou X, Hovell CJ, Pawley S, et al. Expression of matrix metalloproteinase-2 and -14 persists during early resolution of experimental liver fibrosis and might contribute to fibrolysis. Liver Int 2004;24:492–501.

38. Luo L, Zhou A. Antifibrotic activity of anisodamine in vivo is associated with changed intrahepatic levels of matrix metalloproteinase-2 and its inhibitor tissue inhibitors of metalloproteinases-2 and transforming growth factor beta1 in rats with carbon tetrachloride-induced liver injury. J Gastroenterol Hepatol 2009;24:1070–1076.

39. Xu GF, Li PT, Wang XY, et al. Dynamic changes in the expression of matrix metalloproteinases and their inhibitors, TIMPs, during hepatic fibrosis induced by alcohol in rats. World J Gastroenterol 2004;10:3621–3627.

40. Lin HC, Yang YY, Tsai TH, et al. The relationship between endotoxemia and hepatic endocannabinoids in cirrhotic rats with portal hypertension. J Hepatol 2011;54:1145–1153.

41. Murphy FR, Issa R, Zhou X, et al. Inhibition of apoptosis of activated hepatic stellate cells by tissue inhibitor of metalloproteinase-1 is mediated via effects on matrix metalloproteinase inhibition: implications for reversibility of liver fibrosis. J Biol Chem 2002;277:11069–11076.

42. Liu X, Hu H, Yin JQ. Therapeutic strategies against TGF-beta signalling pathway in hepatic fibrosis. Liver Int 2006;26:8–22.

43. Díaz-Gil JJ, García-Monzón C, Rúa C, et al. The anti-fibrotic effect of liver growth factor is associated with decreased intrahepatic levels of matrix metalloproteinases 2 and 9 and transforming growth factor beta 1 in bile duct-ligated rats. Histol Histopathol 2008;23:583–591.

44. Caraceni P, Viola A, Piscitelli F, et al. Circulating and hepatic endocannabinoids and endocannabinoid-related molecules in patients with cirrhosis. Liver Int 2010;30:816–825.

45. Munoz-Luque J, Ros J, Fernandez-Varo G, et al. Regression of fibrosis after chronic stimulation of cannabinoid CB2 receptor in cirrhotic rats. J Pharmacol Exp Ther 2008;324:475–483.

46. Patsenker E, Stoll M, Millonig G, et al. Cannabinoid receptor type I modulates alcohol-induced liver fibrosis. Mol Med 2011 (e-pub ahead of print).

47. Trebicka J, Racz I, Siegmund SV, et al. Role of cannabinoid receptors in alcoholic hepatic injury: steatosis and fibrogenesis are increased in CB2 receptor-deficient mice and decreased in CB1 receptor knockouts. Liver Int 2011;31:860–870.

48. Tam J, Liu J, Mukhopadhyay B, et al. Endocannabinoids in liver disease. Hepatology 2011;53:346–355.

49. Tam J, Vemuri VK, Liu J, et al. Peripheral CB1 cannabinoid receptor blockade improves cardiometabolic risk in mouse models of obesity. J Clin Invest 2010;120:2953–2966.